

# Investigating the Phosphine Chemistry of Se Precursors for the Synthesis of PbSe Nanorods

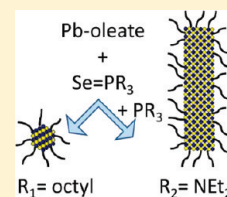
Weon-kyu Koh,<sup>†</sup> Youngmin Yoon,<sup>†</sup> and Christopher B. Murray<sup>\*,†,‡</sup>

<sup>†</sup>Department of Chemistry and <sup>‡</sup>Department of Materials Science and Engineering, University of Pennsylvania, Philadelphia, Pennsylvania 19104, United States

## S Supporting Information

**ABSTRACT:** We studied the role of different Se precursors for PbSe nanorod (NR) synthesis, focusing on phosphine chemistry to understand precursor decomposition. After characterizing the morphology of PbSe nanocrystals (NCs) and NRs with absorption spectra and TEM analyses, we used <sup>31</sup>P NMR to correlate morphology with precursor decomposition during synthesis. While spherical PbSe NCs can be produced with a trioctylphosphine selenide (TOPSe)-based synthesis even at low temperatures (50–60 °C) or without free phosphine, PbSe NRs are more sensitive to their reaction conditions. At lower temperatures, tris(diethylamino)phosphine selenide (TDPSe) does not show any evidence of Se precursor decomposition, and the presence of amine-based free phosphine in the Se precursor affects the morphology of PbSe NRs dramatically. Further TGA-MS analysis implies that TDP accelerates precursor decomposition and morphology evolution by releasing amine species. A control experiment that added amine into both TOPSe and TDPSe with no free phosphine-based reactions shows amine species enhance the attachment process and morphology change.

**KEYWORDS:** colloids, nanocrystals, nanorods, semiconductors, precursors



## INTRODUCTION

Colloidal nanocrystals (NCs) have been investigated with good control of size and morphology,<sup>1</sup> opening electrical and optical applications such as field-effect transistors<sup>2</sup> and photovoltaics.<sup>3</sup> However, the mechanism of NC growth was not fully understood because of the complexity of the colloidal system and the vigorous/air-sensitive synthesis conditions. Although several groups have demonstrated chemical analyses to understand the surface chemistry of NCs or the mechanism of NC growth,<sup>4–7</sup> their studies have mostly focused on the spherical NC system. Another limitation involves the impurities of trioctylphosphine (TOP) or trioctylphosphine oxide (TOPO), which actually affect precursor decomposition, morphology, and properties of the products,<sup>8–10</sup> making it difficult to understand the mechanism. Recently, we reported the synthesis of PbSe nanorod (NR) using tris(diethylamino)phosphine selenide (TDPSe) instead of commonly used TOPSe for spherical NCs, while keeping other reaction conditions such as Pb oleate and temperature the same as for the synthesis of spherical PbSe NCs;<sup>11</sup> this implies that the phosphine selenide precursor has an important role in morphology control. Given that most anisotropic Pb salt nanomaterials are understood as oriented attachment, which still cannot fully explain this precursor-dependent shape evolution,<sup>12,13</sup> it is important to understand the importance of precursor chemistry to produce high quality anisotropic nanomaterials.

Here, we studied the precursor decomposition of PbSe NRs using TDPSe and compared them to the precursor decomposition of TOPSe-based spherical PbSe NCs, with a focus on how different reaction temperatures and precursor conditions affect the decomposition of precursors. We performed <sup>31</sup>P NMR experiments to compare the decomposition of TOPSe and

TDPSe to correlate with the morphologies of PbSe NCs, which are confirmed by absorption spectra and TEM. TGA/TGA-MS demonstrates the possible chemical species released during the reaction, and further control experiments support the additive effect of this species using TEM and <sup>31</sup>P NMR analyses. Details of the experiment, result analysis, and discussion are presented.

## EXPERIMENTAL SECTION

**Chemicals.** All manipulations were carried out using standard Schlenk line techniques under dry nitrogen. Trioctylphosphine (TOP, Strem, 97%), tris(diethylamino)phosphine (TDP, Aldrich, 97%), oleic acid (OA, Aldrich, 90%), 1-octadecene (ODE, Aldrich, 90%), amorphous selenium shots (Se, Aldrich, 99.999%), and lead(II) oxide (PbO, Aldrich, 99.9%), lead acetate trihydrate (PbAc<sub>2</sub>·3H<sub>2</sub>O, Fisher, 99.999%), diphenylphosphine (DPP, Aldrich, 98%), toluene-d<sub>8</sub> (Aldrich, 99.6%), CDCl<sub>3</sub> (Aldrich, 99.8%), and trimethyl phosphate (TMP, Aldrich, 99%) were used as purchased without further purification. Anhydrous ethanol, chloroform, acetone, hexane, and tetrachloroethylene (TCE) were purchased from various sources. To prepare 1.0 M stock solutions of TOPSe or TDPSe, 0.786 g of Se was dissolved in 10 mL of TOP or TDP. To prepare neat TOPSe or TDPSe solutions, TOP or TDP and Se were combined by 1:1 mol ratio and stirred overnight in a nitrogen filled glovebox.

**Temperature Dependence of the Decomposition of Se Precursors.** Typically, 0.22 g of PbO was dissolved in 5 mL ODE in the presence of 1 mL OA. After drying under nitrogen at 150 °C for 30 min, the solution was heated or cooled to desired temperature, and neat or 1 M Se precursor was injected under vigorous stirring (1:1 mol ratio of

**Received:** November 18, 2010

**Revised:** January 10, 2011

**Published:** March 09, 2011

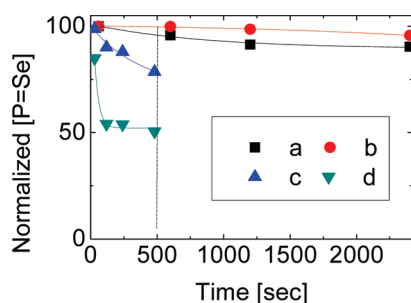


**Figure 1.** Plot for decomposition of (a) 1 M TOPSe and (b) 1 M TDPSe at 50–60 °C and (c) 1 M TOPSe and (d) 1 M TDPSe at 150–160 °C. Dashed line shows conventional PbSe NC growth time limit with further growth providing poor monodispersity of NC products. Data was obtained from integration of  $^{31}\text{P}\{^1\text{H}\}$  NMR peaks, which had less than 5% error.

Pb:Se). Aliquots of the reaction solution was taken from the reaction flask and monitored by absorption spectra or  $^{31}\text{P}\{^1\text{H}\}$  NMR spectra.

**Free Phosphine Effect of the Decomposition of Se Precursors.** The reaction condition was the same as the temperature-dependence experiment. When neat Se precursor was used, the overall concentration was corrected for by the purity of the phosphine source by dilution with ODE.

**Amine Effect of the Decomposition of TDPSe.** For the TDPSe and diethylamine mixture, 1 mmol of TDPSe and 1 mmol of diethylamine is mixed and diluted to 3 mL by ODE as a solvent. For the Pb oleate, TDPSe, and diethylamine mixture, 0.22 g of PbO and 1 mL OA were added and diluted to 3 mL by ODE to keep the overall concentration.

**Sample Characterization.** Transmission electron microscopy (TEM) and high-resolution TEM were carried out by using a JEOL JEM 1400 and a 2010F at 120 and 200 kV, respectively. Samples for TEM images were prepared by dropping a solution on a 300 mesh carbon-coated copper grid and allowing the solvent to evaporate at room temperature. Absorption spectra were measured on a Cary 5000 UV–vis-IR spectrophotometer or QualitySpec Pro Vis/NIR spectrometer at room temperature. All optical experiments were carried out in the solvent TCE.  $^{31}\text{P}\{^1\text{H}\}$  NMR spectra were recorded on a Bruker DMX 360 NMR spectrometer, with proton decoupling. The chemical shifts ( $\delta$ ) are given in parts per million relative to an external standard  $\text{H}_3\text{PO}_4$  (0 ppm) and an internal standard TMP (3.0 ppm).<sup>4</sup> To quantize the ingredients of samples, 10  $\mu\text{L}$  of TMP was added into 0.5 mL of aliquot then diluted to 1 mL by  $\text{CDCl}_3$ . NMR integration of each peak was compared to the given quantity of TMP. Thermogravimetric analysis (TGA) was performed with a heating rate of 10 °C/min under  $\text{N}_2$  on a Thermaladvantage Q600 thermal analyzer connected to a quadrupole mass spectrometer (Pfeiffer Vacuum Thermostar GSD301T).

## RESULTS AND DISCUSSION

**Temperature Effect.** Figure 1 and Figure S2 of the Supporting Information (hereafter to Figure S6 reference raw NMR data) show that TOPSe-based synthesis decomposes more Se precursor than TDPSe-based synthesis at 50–60 °C by monitoring the decrease in TOPSe/TDPSe areas via  $^{31}\text{P}\{^1\text{H}\}$  NMR. In particular, TOPSe-based synthesis at these low temperatures is reported to form PbSe magic size clusters,<sup>8</sup> which appear in their absorption spectra (Figure 2a). However, TDPSe-based synthesis decomposes more Se precursor than TOPSe-based synthesis under normal synthetic conditions of PbSe NCs (150–160 °C) on the basis of  $^{31}\text{P}\{^1\text{H}\}$  NMR spectra. These results are confirmed by absorption spectra; at lower temperature, TOPSe-based synthesis

gives peak evolution during the reaction time (Figure 2a), while TDPSe-based synthesis does not change the absorption spectrum at all (Figure 3a). It is possible that the larger cone angle of TDPSe suppresses the decomposition at low temperature by steric hindrance around the Se atom in contrast to the reported formation of magic size clusters using TOPSe.<sup>8</sup> However, this does not explain why TDPSe-based synthesis shows more decomposition of precursor at higher temperature; this leads us to a further investigation of the free phosphine effect of precursor decomposition.

**Free Phosphine Effect.** While many metal chalcogenide NC syntheses use extra free phosphine in the Se precursor solution, most reports on the NC synthesis mechanism relied on neat phosphine selenide precursor for simplicity.<sup>4,5,8</sup> Indeed, metal chalcogenide spherical NCs have no evidence of free phosphine effect on their synthesis, as confirmed by TEM in panels (a) and (b) of Figure 4. For spherical NCs, we found that their synthesis form spherical products with or without extra free phosphine. However, we found that free phosphine actually has an important role in the morphology control of nonspherical PbSe. TEM shows that 1 M TDPSe makes PbSe NR, but neat TDPSe produces isotropic particles or attached particles but without rod-morphology (Figure 4c and d). Absorption spectra also confirm the morphology-shaping effect of free phosphine, showing similar spectra for TOP-based synthesis (Figure 5a and b) but different pattern of spectra for TDP-based synthesis (Figure 5c and d). We also performed  $^{31}\text{P}\{^1\text{H}\}$  NMR to quantitatively compare the effect of free phosphine in PbSe synthesis at normal conditions (150–160 °C). Neat TOPSe and 1 M TOPSe give 12% and 11% decomposition of initial Se precursor, respectively (Figure S3a,b of the Supporting Information). Neat TDPSe gives 7% decomposition of the initial precursor, which is similar to that of TOP-based synthesis (Figure S3c of the Supporting Information). However, 1 M TDPSe gives 38% decomposition yield, implying that TDP accelerates the precursor decomposition (Figure S3d of the Supporting Information). Thus, we can conclude that the presence of free TDP plays a critical role in the higher precursor decomposition and morphology control in PbSe nanorod synthesis.

**Possible Mechanism of Free Phosphine Effect.** This section explores how free TDP in PbSe NR synthesis may play such an important role. Because the P–N bond of TDP is weaker than P–C bond of TOP, the P–N bond may easily cleave to give amine species under various conditions such as nucleophile attack or EI-MS ionization.<sup>14–16</sup> To confirm the release of amine, we monitored the decomposition of free phosphine in the TDPSe-based synthesis using TGA-MS. One M TDPSe in TDP solution shows a possible  $\text{NET}_2^+$  peak ( $m/z = 72$ ) during the heating process, which can be from either the release of  $\text{NET}_2$  or the fragmentation of vaporized TDP above 150 °C (Figure 6a and b). Running the same experiment with neat TDPSe solution, TGA-MS produces the  $\text{NET}_2^+$  peak at a higher temperature (above 220 °C) with much less ion intensity of mass decomposition than with 1 M TDPSe in TDP solution (Figure 6c,d). Considering that there is little amount of TDP in neat TDPSe solution, the peak at  $m/z = 72$  may be assigned as diethylamine released from either residual TDP or from evaporated TDPSe.

The release of  $\text{NET}_2$  at high temperatures from free phosphine can explain why PbSe NR synthesis is not accelerated at lower temperature (Figures 1b and 3a), while free phosphine accelerates the precursor decomposition at higher temperature with the release of amine (Figures 1d, and 3b). To confirm the amine effect of precursor decomposition, we mixed neat TDPSe and

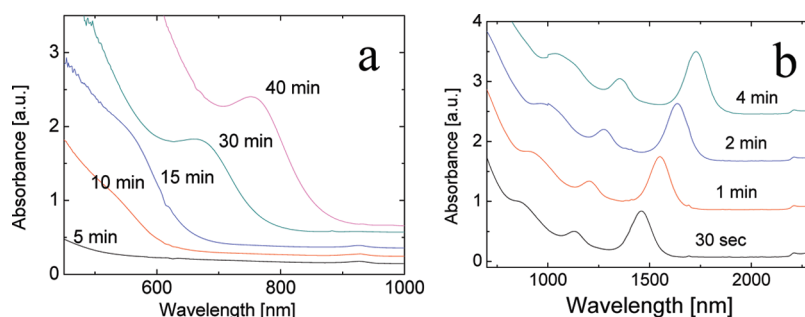


**Figure 2.** Absorption spectra of Pb oleate and 1 M TOPSe at (a) 50–60 °C and (b) 150–160 °C.

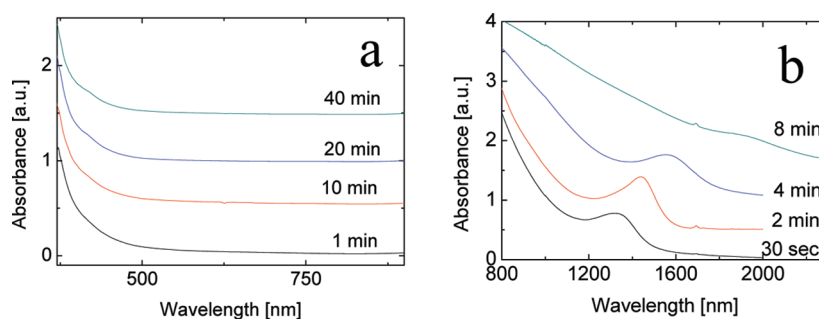


**Figure 3.** Absorption spectra of Pb oleate and 1 M TDPSe at (a) 50–60 °C and (b) 150–160 °C. Panel (b) is reproduced with permission from ref 11.

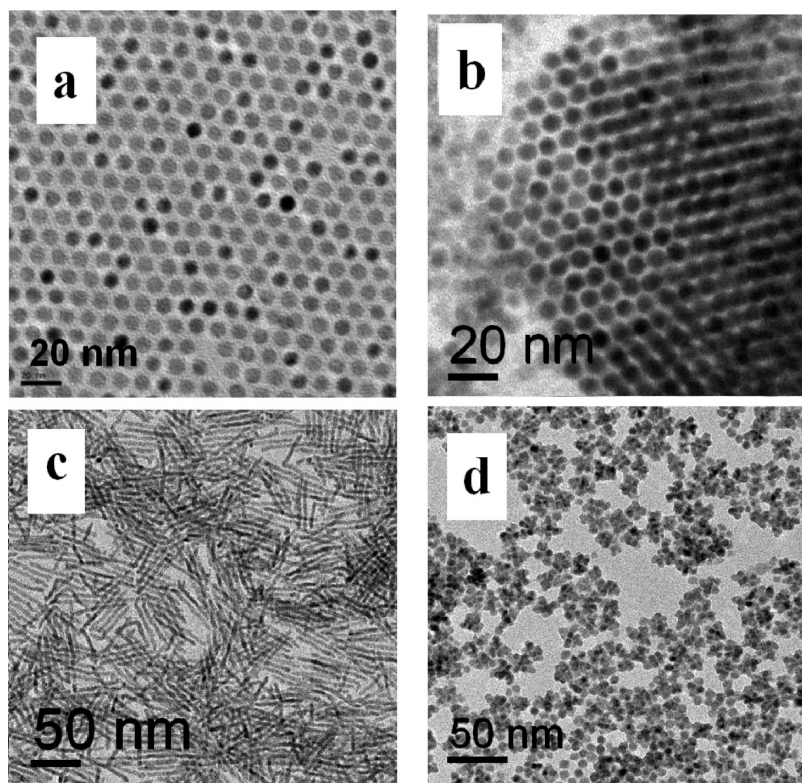


**Figure 4.** TEM images of spherical PbSe NCs (a, 7.5 nm) with 1 M TOPSe vs (b, 7.0 nm) with neat TOPSe and those of PbSe NRs (c,  $40 \times 4 \text{ nm}^2$ ) with 1 M TDPSe and (d) with neat TDPSe. All reactions were done at 150–160 °C.

diethylamine by 1:1 mol ratio in ODE as a solvent at 50–60 °C. After 40 min, 21.9% of TDPSe was decomposed with diethylamine, but less than 1% of TDPSe was decomposed without

diethylamine (Figure S4 of the Supporting Information). Also, the mixture of lead oleate, TDPSe, and diethylamine by 1:1:1 mol ratio in ODE as a solvent at 50–60 °C results in the



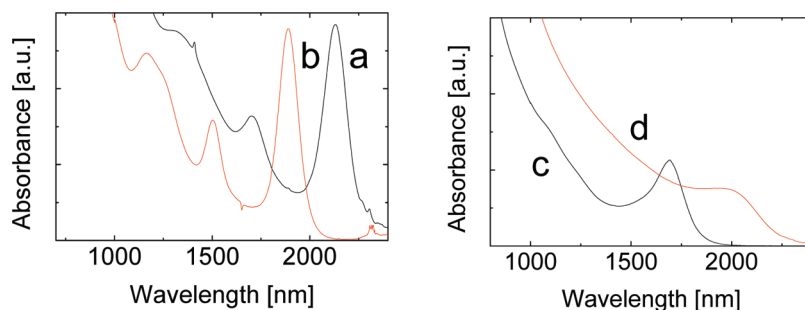


**Figure 5.** Absorption spectra of spherical PbSe NCs (a) with free TOP vs (b) without free TOP and those of PbSe NRs (c) with free TDP and (d) without free TDP. All reactions were done at 150–160 °C.

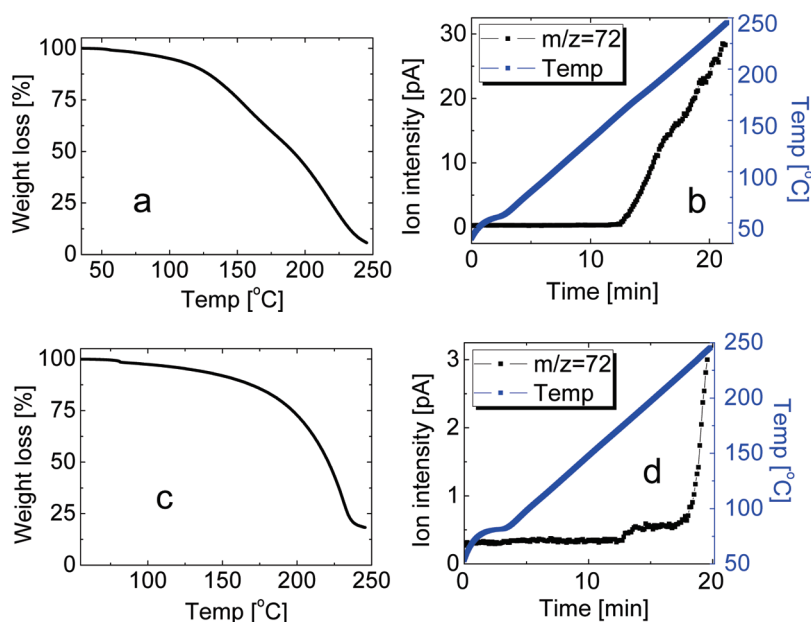


**Figure 6.** (a) TGA and (b) TGA-MS of 1 M TDPSe in TDP solution (starting mass = 18.4020 mg). (c) TGA and (d) TGA-MS of neat TDPSe solution (starting mass = 20.9930 mg).

decomposition of TDPSe by 15.7%, while the same mixture without diethylamine causes the decomposition of TDPSe by 3.6% (Figure S5 of the Supporting Information). It is well-known that amines can affect precursor decomposition and crystal growth for CdSe and InP NCs.<sup>17–19</sup> Although the exact role of amines in the precursor decomposition and crystal growth is not yet fully understood, as seen in the different effects of long chain amine additives for InP NCs described by Peng<sup>18</sup> and Bawendi<sup>19</sup> groups, our result with short chain amine indicates enhanced precursor decomposition. We speculate that the difference between the effects of long chain and short chain amines may be due to their differences in steric hindrance, with diethylamine being less sterically hindered and thus more activating.

**Role of Amine for the Morphology of PbSe.** After confirming the effect of diethylamine for precursor decomposition, we checked its effect on PbSe morphology by adding a minimum quantity of diethylamine to the growth solution by diluting diethylamine in octadecene (ODE) solvent. Diethylamine was minimized by diluting in ODE because the direct injection of diethylamine into the reaction solution gave an uncontrollable reaction that immediately turned the solution black at the typical reaction temperature of PbSe NR (150–160 °C). For 1 mmol of

PbO (0.22 g, same scale as the other reactions), 0.2 mL of 10% by volume of diethylamine in ODE was injected after injection of neat TOPSe or TDPSe at 170 °C. The precursor decomposition with diethylamine is similar to the reactions without diethylamine: 10% for TOPSe and 3% for TDPSe, respectively (Figure S6 of the Supporting Information). In this case, we do not observe rate enhancement with added amine probably because of the small quantity of diethylamine, in which the mole ratio of Pb: diethylamine is  $\sim 1:0.2$ . However, the morphologies of final products are quite different by TEM. TOPSe-diethylamine produces more homogeneously attached particles (Figure 7a), and TDPSe-diethylamine starts to provide thin and long rod-like products (Figure 7b).

It is well-known that the amine group is weakly binding on the surface of PbSe nanocrystals, especially on {111} facets.<sup>12</sup> Oriented attachment is found in many cases, especially when the highly energetic facets are attached to minimize the surface energy of the particles by making a single crystalline.<sup>12,13,20</sup> It is possible that released amine species from TDP could accelerate the attachment process by removing {111} facets of PbSe, especially when short-chain and low boiling point diethylamine is present in the growth solution. However, it is still critical to

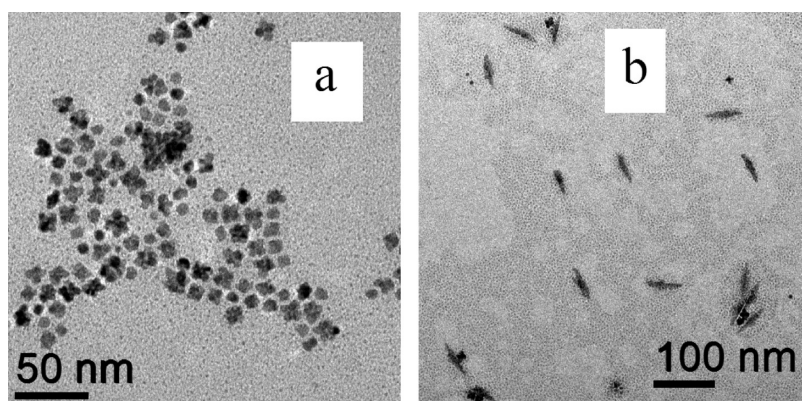


**Figure 7.** TEM images of reaction products from Pb oleate and (a) TOPSe-diethylamine and (b) TDPSe-diethylamine at 150–160 °C for 5 min.

have TDPSe as a Se precursor to produce anisotropic PbSe nanorod because TOPSe-diethylamine only enhances the attachment process to produce branched structures.

At reaction temperatures below 100 °C, the Pb oleate, TDPSe, and diethylamine in ODE solution did not turn black, and there was no PbSe product. This suggests that although NMR data show diethylamine increases the decomposition of TDPSe, it might be possible that triggering the intermediate to produce final PbSe requires higher growth temperatures than the decomposition temperature. With growth temperature at 100–110 °C, mainly tiny particles are produced both with and without diethylamine (Figure S8a of the Supporting Information). Interestingly, a small portion of disk-shaped PbSe was observed in TEM images when diethylamine was added during growth (Figure S8b of the Supporting Information), implying that diethylamine effect varies depending on growth temperatures. A more detailed mechanism of PbSe NR formation and Se precursor phosphine chemistry is underway.

## CONCLUSIONS

In conclusion, we studied the morphology of PbSe NCs by understanding precursor chemistry with an emphasis on how different phosphine selenide systems react to shape the final product. Temperature dependence of precursor decomposition implies the effect of steric hindrance for phosphine selenide precursors. TEM images and absorption spectra show consistent results that free phosphine is critical to induce anisotropic morphology of PbSe NRs.  $^{31}\text{P}$  NMR supports the effect of free phosphine for precursor decomposition of PbSe, and TGA-MS provides evidence of amine release from TDP. A further control experiment with added amine species demonstrates a possible origin of the morphology change in the growth of PbSe nanocrystal. We hope this report advances the understanding of both the fundamental science of phosphine chemistry and the chalcogenide-based semiconductor NC synthesis.

## ASSOCIATED CONTENT

**S Supporting Information.** Supplementary figures as described in the text. This material is available free of charge via the Internet at <http://pubs.acs.org>.

## AUTHOR INFORMATION

**Corresponding Author**

\*E-mail: [cbmurray@sas.upenn.edu](mailto:cbmurray@sas.upenn.edu).

## ACKNOWLEDGMENT

We acknowledge financial support from the NSF through DMS-0935165 (C.B.M. and W.-k.K.). This research was partially supported by the Nano/Bio Interface Center through the National Science Foundation (NSEC DMR08-32802). The authors thank George Furst and Jun Gu for support in NMR spectroscopy, Andrew McGhie for help with the TGA experiment, and Danielle Reifsnnyder for helpful advice regarding the manuscript.

## REFERENCES

- (1) Murray, C. B.; Kagan, C. R.; Bawendi, M. G. *Annu. Rev. Mater. Sci.* **2000**, *30*, 545–610.
- (2) Talapin, D. V.; Murray, C. B. *Science* **2005**, *310*, 86–89.
- (3) Huynh, W. U.; Dittmer, J. J.; Alivisatos, A. P. *Science* **2002**, *295*, 2425–2427.
- (4) Liu, H.; Owen, J. S.; Alivisatos, A. P. *J. Am. Chem. Soc.* **2007**, *129*, 305–312.
- (5) Steckel, J. S.; Yen, B. K. H.; Oertel, D. C.; Bawendi, M. G. *J. Am. Chem. Soc.* **2006**, *128*, 13032–13033.
- (6) Moreels, I.; Fritzinger, B.; Martins, J. C.; Hens, Z. *J. Am. Chem. Soc.* **2008**, *130*, 15081–15086.
- (7) Tracy, J. B.; Crowe, M. C.; Parker, J. F.; Hampe, O.; Fields-Zinna, C. A.; Dass, A.; Murray, R. W. *J. Am. Chem. Soc.* **2007**, *129*, 16209–16215.
- (8) Evans, C. M.; Evans, M. E.; Krauss, T. D. *J. Am. Chem. Soc.* **2010**, *132*, 10973–10975.
- (9) Wang, F.; Tang, R.; Kao, J. L. F.; Dingman, S. D.; Buhro, W. E. *J. Am. Chem. Soc.* **2009**, *131*, 4983–4994.
- (10) Morris-Cohen, A. J.; Donakowski, M. D.; Knowles, K. E.; Weiss, E. A. *J. Phys. Chem. C* **2010**, *114*, 897–906.
- (11) Koh, W.; Bartnik, A. C.; Wise, F. W.; Murray, C. B. *J. Am. Chem. Soc.* **2010**, *132*, 3909–3913.
- (12) Cho, K. S.; Talapin, D. V.; Gaschler, W.; Murray, C. B. *J. Am. Chem. Soc.* **2005**, *127*, 7140–7147.
- (13) Schliebe, C.; Juarez, B. H.; Pelletier, M.; Jander, S.; Greshnykh, D.; Nagel, M.; Meyer, A.; Foerster, S.; Kornowski, A.; Klinke, C.; Weller, H. *Science* **2010**, *329*, 550–553.
- (14) Raouafi, N.; Khelifi, A.; Boujlél, K.; Benkhoud, M. L. *Heteroat. Chem.* **2009**, *20*, 272–277.
- (15) Habicher, W. D.; Pawelke, B.; Bauer, I.; Yamaguchi, K.; Kósa, C.; Chmela, Š.; Pospíšil, J. *J. Vinyl Addit. Technol.* **2001**, *7*, 4–18.
- (16) Zhou, J.; Chen, R.; Yang, X. *Heteroat. Chem.* **1998**, *9*, 369–375.
- (17) Pradhan, N.; Reifsnnyder, D.; Xie, R.; Aldana, J.; Peng, X. *J. Am. Chem. Soc.* **2007**, *129*, 9500–9509.
- (18) Xie, R.; Battaglia, D.; Peng, X. *J. Am. Chem. Soc.* **2007**, *129*, 15432–15433.
- (19) Allen, P.; Walker, B.; Bawendi, M. G. *Angew. Chem., Int. Ed.* **2010**, *49*, 760–762.
- (20) Penn, R. L.; Banfield, J. F. *Science* **1998**, *281*, 969–971.